

Studying Methods of Estimating Heat Generation at Three Different Zones in Metal Cutting: A Review of Analytical models

Ajay Goyal^{#1}, Shailendra Kumar^{*2}, Suresh Dhiman^{*3}, Rajesh Kumar Sharma^{*4}

^{#1}Assistant Professor, Mechanical Engineering Department, Mangalayatan University, Aligarh, Uttar Pradesh, India

^{*2}M. Tech. student, National Institute of Technology, Hamirpur, Himachal Pradesh, India

^{*3}Assistant Professor, National Institute of Technology, Hamirpur, Himachal Pradesh, India

^{*4}Associate Professor National Institute of Technology, Hamirpur, Himachal Pradesh, India

ABSTRACT: The temperature rise during machining would severely affects the quality of work as well as tool life, if goes beyond a limit. Prior estimation and control of this temperature rise have always being a thrust area for machinists in adopting the optimum machining parameters. Though the temperature rise can be measured experimentally but reliable and time tested mathematical model(s) will serve the purpose in a better way. Mathematical model(s) is handy and economic as compared to experimental methods for set of machining parameters. A number of mathematical methods are developed, and the results have been compared with reality. In this paper efforts have been made to review and systemize the study of all such major analytical methods developed in past to identify the future scope of research. Further, a Comparative study of merits and demerits of experimental methods for measurement of temperature rise developed, in past is tabulated.

Keywords: Analytical models, experimental methods, temperature rise, metal cutting, primary deformation zone, secondary deformation zone, tertiary deformation zone

1. Introduction

It is a well-known fact that a sufficiently large amount of mechanical energy required for metal cutting, is ultimately transformed into heat energy [1], [2], [3]. This heat energy results in the rise in temperature of tool, chip and work piece. The temperature rise affects the machinability, metallurgical, and other properties of work piece, & tool life, if goes beyond a limit. Though the temperature rise is different for different work and tool combinations, it has been well understood that this temperature rise mainly depends upon machining parameters [4] and can be contained by setting machining parameters optimally. Therefore, a prior estimation of temperature rise would be highly beneficial as this will make the task of selecting optimum machining parameters much easier. Researchers concluded that this temperature rise mainly due to three deformation zones namely

primary, secondary, and tertiary deformation zones [5]. Primary deformation zone contributes maximum to temperature rise followed by secondary deformation zone.

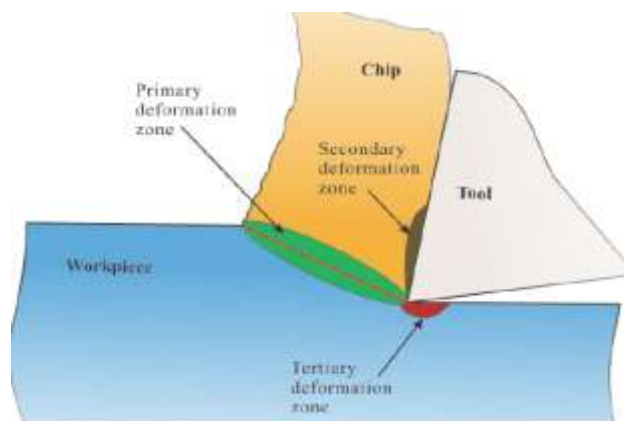


Fig.1 Heat zones in metal cutting [5]

The contribution of tertiary deformation zone does not make significant difference in the temperature rise.

A handy knowledge of heat generation and subsequent temperature rise at various points of tool, chip, and work piece would facilitate in the selection of optimum machining parameters which will result in better machining i.e. enhanced work quality in lesser time, increased tool life, etc. A number of methods for estimation of temperature rise have been developed and tested by researchers. These methods are categorized in two broad areas namely Experimental, and Analytical. Though, the main objective of the paper is the study of analytical methods, still a little focus on Experimental methods will not be beyond the scope of the paper because experimental methods are the ultimate standard for comparison. In this paper, the brief study of experimental methods is followed by a detailed study of analytical models.

I.I Experimental methods

Experimental methods for determining temperature rise in metal cutting are expensive but easy to perform once setup is installed. These methods give direct reading of temperature rise and do not need any input parameters during machining but apparatus needed for measurement of temperature is costly and requires special settings. Results obtained by these methods are near to reality although much accuracy is not desired for number of industrial applications. Installation of special experimental setup for temperature measurement by these methods is a tedious and expensive project itself. To the best of authors knowledge, following seven experimental methods for measurement of temperature rise have been reported in the literature: (1) Thermal paints technique, (2) Thermocouple techniques -Tool-work thermocouple technique, Transverse thermocouple technique, and Embedded thermocouple technique, (3) Infrared radiation pyrometer technique, (4) Optical infrared radiation pyrometer technique, (5) Infra-red photography, (6) Fine powder techniques, (7) Metallographic methods. A comparative study of merits and demerits of these experimental methods is tabulated in table 1.

I.II ANALYTICAL METHODS

In contrast with the experimental methods, analytical methods do not require any special experimental setup. In analytical methods the result(s) can be obtained by using computational software (like ANSYS®, MATLAB®, ANOVA®, etc.) along with few input data. This input data normally adopted from the experimental investigations (uses setup which is easy to install) carried out during machining of material. A little compromise on accuracy makes the analytical methods very fast and extensive. That's why, now day's industries are relying more on analytical models rather experimental. In this paper, an effort has been made to review all analytical models in past.

Idiom 'Rome was not built in a day' is also applicable to the development of analytical models. Rapid development in computer science gives the impetus to the development of analytical models. The pioneer work of Rosenthal [6], Blok [7], and Jaeger [8] during 1930's and 1940's has been the basis for further investigation and inspired the next generation to work in this field. The major work in this field is observed as the extension of Jaeger's [8], [9] approximate solutions of a moving-band heat source for the chip and a stationary rectangular heat source for the tool in metal cutting. In order to systemize the study, first we reviewed the effect of primary, secondary, and tertiary heat zone on temperature rise by considering one at a time. The combined effect of primary and secondary heat zone on temperature rise is studied afterwards.

II. Study of temperature rise due to Primary Deformation Zone

Most of the scientists have tried to develop the model(s) by considering shear plane as a moving band of heat source. For the ease of understanding, the research is further divided in two groups, the first group of scientists treated work piece and chip as different entities, while the second group treated work piece, and chip as single entity. Here, we first discuss the research carried out by former group followed by the later.

II.1 Research by assuming work piece and chip as different entity

It is observed that the scientists whose research area is falling in this category made a common assumption that work piece is sliding relative to chip. They applied Blok's model [7] for prediction of sharing of heat evolved between chip and work piece due to shearing action during metal cutting. Different models are discussed below in chronological order:

II.1.1 Loewen and Shaw's model

Figure 2 encompasses Loewen and Shaw's model [10]. They used the concept of Blok's heat partition [7], Jaeger's solution for the moving slider problem [8], and Piispanen's sliding deck of cards [11], with the following major assumptions:

- Adiabatic shear plane and hence no heat flow from work piece to the chip,
- Moving heat source with a shear velocity

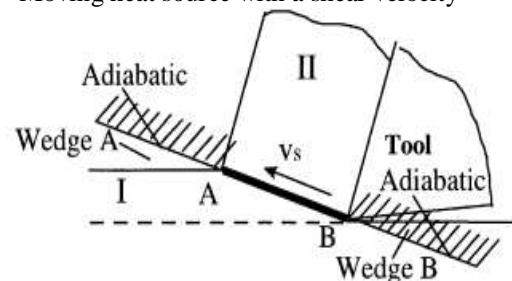


Fig. 2 Schematic diagram of Loewen and Shaw's model [10]

The average temperature on either side of shear plane was calculated using solutions of moving plane heat source after Carslaw and Jaeger's theory [9].

This model could not give accurate results for distribution of temperature in the chip during its formation.

II. I.II Leone's Model

Leone's [12] model (Fig.3) is similar to Loewen and Shaw's model [10] which has been further simplified by considering shear angle as zero i.e. this model considered the moving heat source parallel to cutting

velocity and simplified the tedious calculations to simple frictional sliding contact calculations. The author also assumed that shear plane is moving with cutting velocity however, this model was also not found accurate in prediction of results.

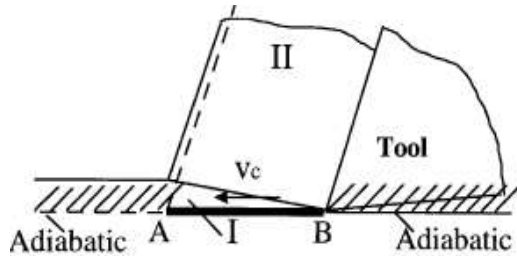


Fig. 3 Schematic diagram of Leone's model [12]

The major common drawback observed in both the above discussed models was non-consideration of the material flow while machining.

II.I.III Weiner's model

The common drawback of previous two models was overcome by Weiner's model [13] which is schematically presented in Fig.4. He used the concept of three models namely Loewen and Shaw's model [10]; Leone's model [12], and Trigger and Chao's model [14] (discussed later in section 2.2.1), with the following major assumptions:

- Machined and un machined surface considered to be adiabatic
- Moving heat source is inclined at shear angle
- Heat source is moving with cutting velocity so the heat source moves into the material, not in an imaginary space.
- Flow of chip to be perpendicular to shear plane

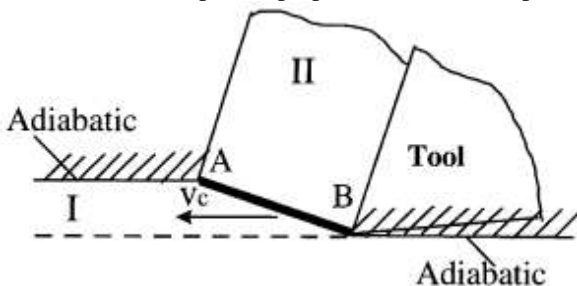


Fig. 4 Schematic diagram of Weiner's model [13]

The model used partial differential equation for conduction of heat while earlier discussed models used Jaeger's solution for modeling. The results were improper due to the large number of assumptions.

II.I.IV Dutt and Brewer's model

Dutt and Brewer [15] model (Fig.5) used finite difference methods; moreover the authors developed equations of temperature distribution for chip, tool, and

work piece as separate entities and then combined them to form equations for determining temperature distribution of the whole system using some boundary conditions. They considered side boundaries of chip, machined and unmachined surface as adiabatic boundaries. The heat source was considered to be moving at cutting velocity.

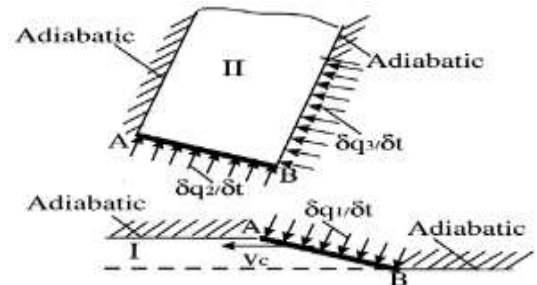


Fig. 5 Schematic diagram of Dutt and Brewer's model [15]

II.I.V. Dawson and Malkin's model

Dawson and Malkin [16] got inspiration from Weiner's model [13] and prepared almost same model (Fig.6) but with a different approach. They assumed boundaries to be convective instead of adiabatic & used Finite Element Analysis to predict distribution of temperature at various zones of heat generation. The model still gave approximate results.

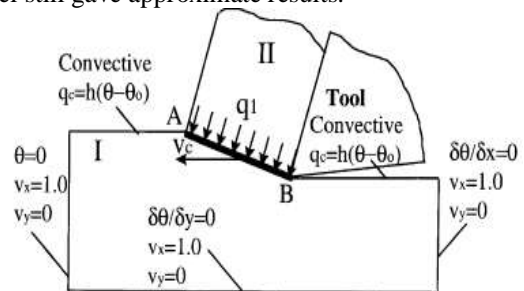


Fig.6 Schematic diagram of Dawson and Malkin's model [16]

The above discussed models assumed work piece and chip as totally different entities sliding with respect to each other. Though, in early 1950s, Hahn [14], Chao and Trigger [17], Trigger and Chao [18] already reported that work piece and chip act as single entity, where chip is plastically deformed along shear plane. However, at that time the concept could not be accepted and was overlooked by other scientists and they continued the inappropriate use of Blok's model [7]. Later, with the help of modern computational sources the concept was proved correct and scientist community started following it. The concept was further reestablished by Komanduri and Hou [19] at the end of 20th century.

II.II Research by assuming work piece and chip as single entity

The second group of scientist assumed chip and work piece as same entity, where chip is deformed plastically during metal cutting. Major contributions in this field are discussed below:

II.II.1 Trigger and Chao Model:

Trigger and Chao [18] were the first to consider above mentioned approach and directed the research in this area. The main assumptions for the model (Fig.7) are:

- a) Shear plane as moving band heat source
- b) Machined and work surface as adiabatic boundaries, hence no loss of heat and same temperature rise at all points
- c) Heat band is moving with shear velocity

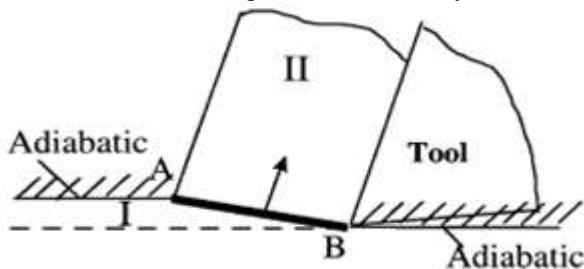


Fig.7 Schematic diagram of Trigger and Chao's model [18]

Average temperature of chip during its formation was expressed by the equation (1):

$$\theta_{avg-chip} = \frac{A[F_c V_c (B_{chip}) - F V_{chip}]}{Jc\rho V_c t_{chip} W} \quad (1)$$

They further modified the equation (1) by eliminating the parameter of latent energy, as expressed in equation (2):

$$\theta_{avg-chip} = (B_{chip}) \frac{F_c V_c - F V_{chip}}{Jc\rho V_c t_{chip} W} \quad (2)$$

The model was able to calculate the average temperature. But it fails to calculate the temperature distribution at different points; the reason might be the lack of computational resources at that time. Further, the assumption that there is no loss of heat from the surfaces and same temperature rise ($\theta_{avg-chip}$) at all points is not realistic and leads to erroneous results.

II.II.II Hahn's model

Figs. 8 and 9 show schematic and mathematical modeling diagram of Hahn's model [14]. This model is based on the same principal as proposed by Trigger and Chao [18]. The difference is that Hahn assumed no boundary conditions and shear plane moving with cutting velocity at oblique angle (ϕ) in an infinite medium.

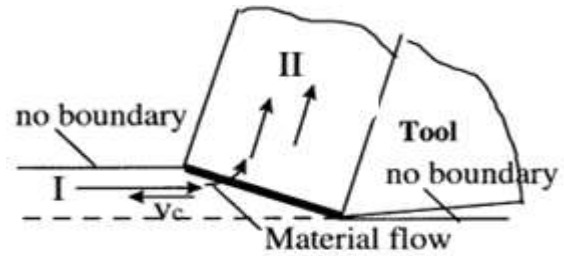
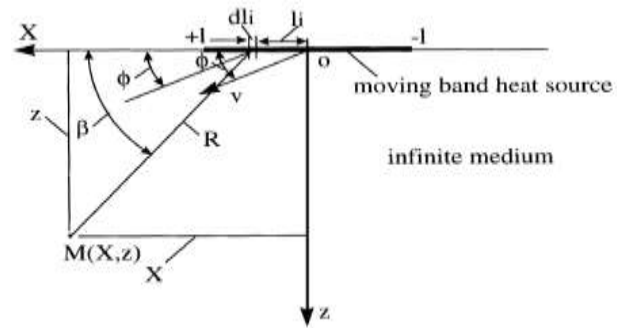


Fig.8 Schematic diagram of Hahn's model [14]

Fig. 9 Mathematical Modeling Diagram of Hahn's Model [14]



Hahn proposed equation (3) for determining temperature rise at any point due to moving band heat source.

$$\theta_M = \frac{q_{shear}}{2\pi k} \int_{-1}^1 e^{-\frac{VR \cos(\beta-\phi)}{2a}} K_0 \left(\frac{VR}{2a} \right) dl_i \quad \text{where} \quad (3)$$

$$R = \sqrt{(X - l_i)^2 + z^2}$$

The equation (3) was further generalized to equation (4) by using $z=0$ (i.e. only temperature rises at heat zone is considered), $\beta = 0$, $\cos(\beta - \phi) = \cos(\phi)$, $R = X - l_i$

$$\theta_M = \frac{q_{shear}}{2\pi k} \int_{-1}^1 e^{-\frac{V(X-l_i)\cos(\phi)}{2a}} K_0 \left(\frac{V(X-l_i)}{2a} \right) dl_i \quad (4)$$

It is interesting to note that substitution of $\phi=90^\circ$ in equation (3), leads to Rosenthal's [6] solution, substitution of $\phi=0^\circ$, leads to Jaeger's [8] solution. Thus equation (3) can be considered as generalized equation for Jaeger [6] and Rosenthal [8] solution.

Non availability of required computational power in 1950s, restricted the Hahn's work in determining temperature distribution at any point due to shear plane for the case $z = 0$. While the relations developed by him could be used for determining temperature rise at any point around the moving heat source. The model is treated as mile stone, and the basis for further developments.

Chao and Trigger [17] notified that it would be appropriate to formulate temperature rise in semi-infinite medium instead of infinite medium because in metal cutting, shear band heat source moves along the boundary

with one end always coinciding with a boundary. While Hahn did not consider the boundary (i.e. $z = 0$), and ended with results lower than intended.

II.II.III Chao and Trigger’s Model

Chao and Trigger [17] (Fig.10) modified Hahn's model [14] by considering a semi-infinite medium by assuming that the temperature at any point (obtained from modified model) to be twice that which will be obtained from Hahn’s model [14]. This is true only for the special case of the heat source moving entirely on the boundary surface of a semi-infinite body. But in reality, only a single point of the band is in contact with the boundary surface.

Loewen and Shaw [10] pointed that Chao and Trigger’s model [17] is not correct as the model shows uniform temperature distribution. Similar to Hahn [14], Chao and Trigger [17] were unable to calculate temperature distribution in the chip and the work piece near the shear zone due to lack of computational software.

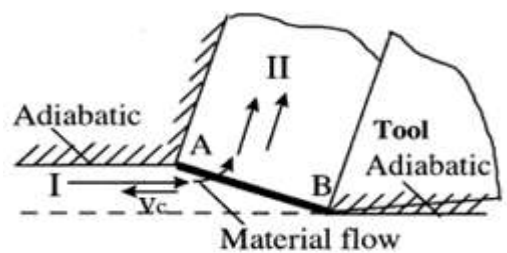


Fig.10 Schematic diagram of Chao and Trigger’s Model [17]

II.II.IV Modified Hahn’s model

Komanduri and Hou [19] further modified Hahn’s model for their modeling on latest computational software and claimed that temperature distribution on chip/ work piece/ tool, could be determined in fraction of minute. Figs. 11 and 12 show schematic of modified Hahn’s model for work side and chip side respectively. Fig. 13 shows oblique band heat source model of modified Hahn’s model in an infinite medium. They developed the model by inclining heat source at an oblique angle, moving at cutting speed along oX direction.

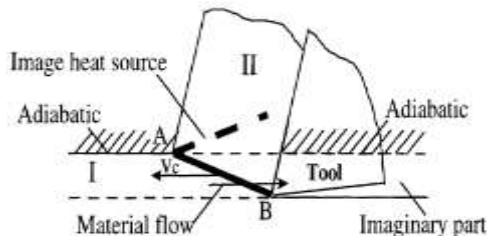


Fig.11 Schematic diagram of modified Hahn’s model for thermal analysis of work [19]

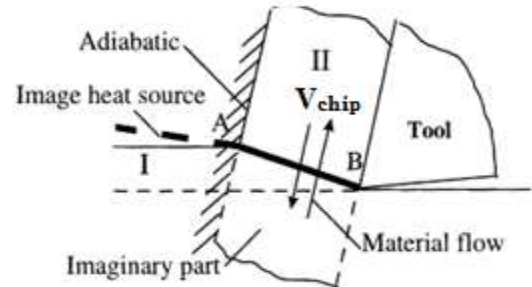


Fig.12 Schematic diagram of modified Hahn’s model for thermal analysis of chip [19]

Komanduri and Hou [19] proposed equation (5) for determination temperature rise at any point $M(X,z)$ around a moving band heat source in an infinite medium which is written below. Like previous models this model also estimates lesser temperature rise than the actual.

$$\theta_M = \frac{q_{shear}}{\pi k} \frac{a}{v \sin \phi} \int_{u=\frac{v(x-L \sin \phi)}{za}}^{\frac{vx}{za}} e^{-u} K_0 \left[\sqrt{u^2 + \frac{v^2}{4a^2} \left(z - \frac{x \sin \phi}{v} \right)^2} \right] du \quad (5)$$

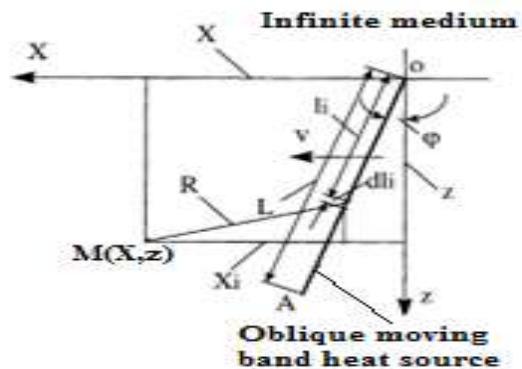


Fig. 13 Schematic diagram of modified Hahn’s model of an oblique band heat source in an infinite medium [19]

Both the concepts of finite medium and semi-infinite medium produced inaccurate results. It indicates that there must also be any other factor left untreated. In the quest of this untreated factor, Komanduri and Hou developed a model [19] by considering a new dimension i.e. image heat source [9] in modified Hahn’s model.

II.II.V Komanduri and Hou’s model

Komanduri and Hou [19] used their modified Hahn’s model [19] as the base for their further investigation of determining temperature rise distribution due to shear plane, at both chip and work piece. Schematic diagrams of the model, for thermal analysis of work side and chip side are shown in Fig. 14 and 15 respectively. Its mathematical modeling diagram is prescribed in Fig.16. They considered the following assumptions:

- (a) Shear plane as infinitely long oblique plane; moving at cutting velocity in a semi infinite medium.
- (b) Work piece and chip as same entity
- (c) Chip is plastically deformed along shear plane in semi infinite medium
- (d) Image heat source of same heat intensity as that of original heat source
- (e) The work material and the chip were extended past the shear plane as an imaginary region for continuity and ease of modeling (Fig.14 and Fig.15)

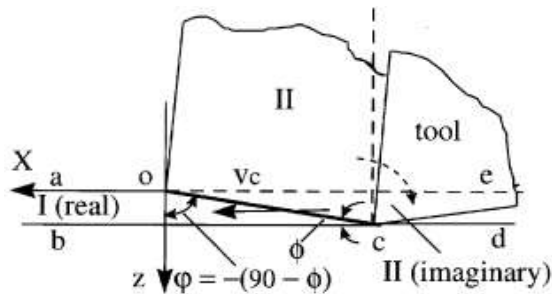


Fig. 14 Schematic diagram of Komanduri and Hou's model for thermal analysis of work [19]

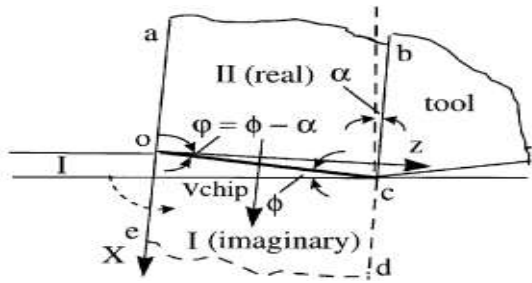


Fig. 15 Schematic diagram of Komanduri and Hou's model for thermal analysis of chip [19]

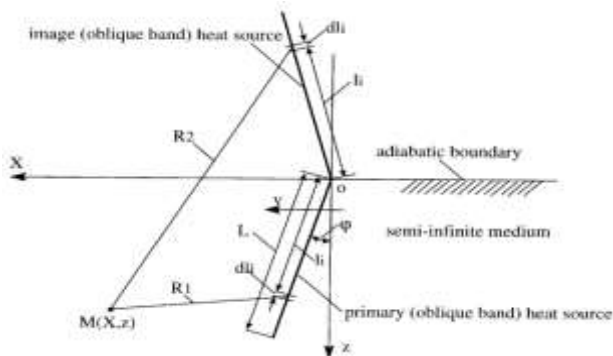


Fig. 16 Komanduri and Hou's model for determining temperature distribution at any point around the moving band heat source in semi-infinite medium [19]

The temperature rise due to real and imaginary heat source at any point M is given by equation (6):

$$\theta_M = \frac{q_{z, shear}}{2\pi k} \int_{l_1=0}^L e^{-(X-l_1 \sin \phi) \frac{v}{2a}} \left\{ K_0 \left[\frac{v}{2a} \sqrt{(X - l_1 \sin \phi)^2 + (z - l_1 \cos \phi)^2} \right] + K_0 \left[\frac{v}{2a} \sqrt{(X - l_1 \sin \phi)^2 + (z + l_1 \cos \phi)^2} \right] \right\} dl_1 \quad (6)$$

Equation (6) can also be used to determine temperature distribution at work surface due to shear plane by replacing ϕ with $(\phi - 90)$. Similarly, for determining distribution of temperature at chip due to shear plane, equation (6) can be used by replacing ϕ with $(\phi - \alpha)$ [19]. Results obtained are considerably satisfactory in nature.

II.II.VI Huang and Liang's model

They modified Komanduri and Hou's model [19] and introduced different models for chip and work piece described here under.

II.II.VI.I Huang and Liang's model for chip side

Schematic, and mathematical model of Huang and Liang [20] for chip side temperature distribution are shown in Fig. 17 and Fig.18 respectively. They considered the same assumptions as Komanduri and Hou [19] except the followings:

- (a) Both boundaries of chip as adiabatic, hence temperature distribution on chip and tool side should be identical.
- (b) Two image heat source of half heat intensity as that of original primary heat source.

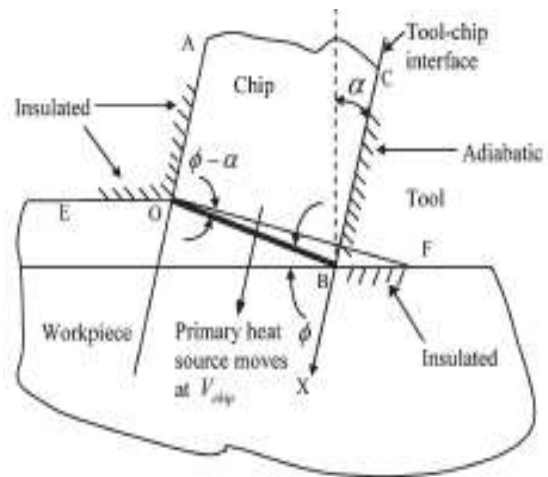


Fig.17 Schematic diagram of Huang and Liang model for thermal analysis of chip [20]

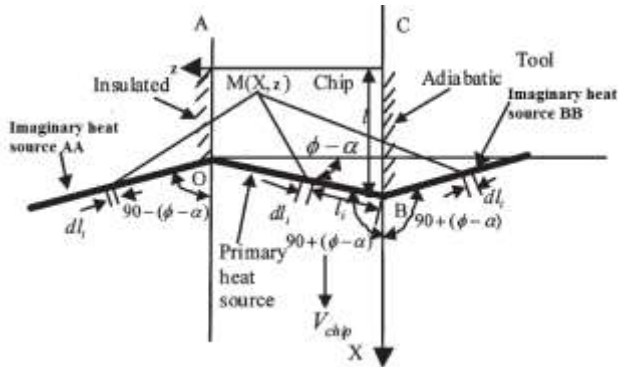


Fig.18 Schematic diagram of Huang and Liang heat transfer model to the chip side [20]

Equation (7) is developed by Huang and Liang for estimation of temperature rise on chip side due to shear heat at any point M:

$$\theta_{chip-shear} = \frac{q_{shear}}{2\pi k_{chip}} \int_0^l \frac{(l-l_i)V_{chip}}{2a_{chip}} \left\{ K_0 \left(\frac{V_{chip}}{2a_{chip}} \sqrt{(l-l_i)^2 + (z-l_i)^2} \right) + \frac{1}{2} K_1 \left(\frac{V_{chip}}{2a_{chip}} \sqrt{(l-l_i)^2 + (2t_{chip}-z-l_i)^2} \right) + \frac{1}{2} K_2 \left(\frac{V_{chip}}{2a_{chip}} \sqrt{(l-l_i)^2 + (z+l_i)^2} \right) \right\} dl_i$$

Where,

$$\begin{aligned} X_i &= l - l_i \sin(\phi - \alpha) \\ Z_i &= l_i \cos(\phi - \alpha) \end{aligned} \quad \text{and} \\ L &= t_c / \sin \phi \quad (7)$$

II.II.VI.II Huang and Liang's model for work piece side

Komanduri and Hou [19] considered the following right part of the work piece next to shear plane 'eocd' (refer Fig.14)) as imaginary and extended it for continuity in their modeling. Huang and Liang [21] modified it by considering boundary conditions of the work piece to be insulated as shown in fig.19. They also considered an imaginary heat source HH with the same heat intensity as that of the primary heat source for their model [21]. Using the model, they developed equation (8) for temperature rise at work piece side:

$$\theta_{work\ piece-shear} = \frac{q_{shear}}{2\pi k_{work\ piece}} \int_0^L e^{-\frac{(x-l_i \sin \phi - VB)V_c}{2a_{work\ piece}}} \left\{ K_0 \left[\frac{V_c}{2a_{work\ piece}} \sqrt{(VB + l_i \cos \phi - X)^2 + (z + l_i \sin \phi)^2} \right] + \left[K_0 \left[\frac{V_c}{2a_{work\ piece}} \sqrt{(VB + l_i \cos \phi - X)^2 + (2t + z - l_i \sin \phi)^2} \right] \right\} dl_i \quad (8)$$

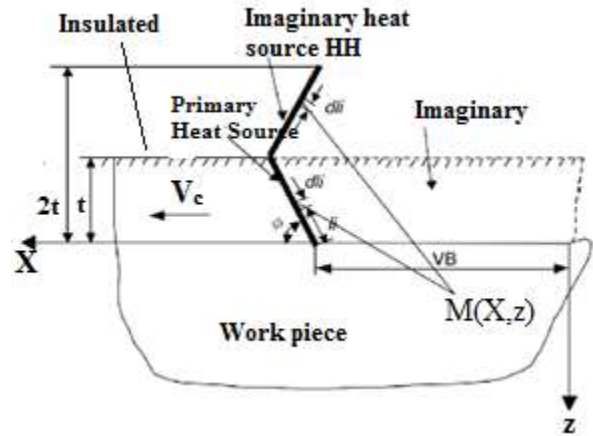


Fig.19 Schematic diagram of Huang and Liang heat transfer model for work piece side [21]

III. Study of temperature rise due to Secondary Deformation Zone

Heat generated due to secondary deformation zone directly affects the rake face of the tool which leads the deterioration of tool surface and thus tool life [10], [18], [22], [23] and [24]. It is inevitable to estimate and check this heat generation at tool-chip interface for increased tool life. Major work in development of analytical methods in this regards are expressed here.

The work of Trigger and Chao [18] was pioneer in the field and similar work was followed by Loewen and Shaw [10]. Both of them considered chip is moving relative to stationary tool at chip velocity and applied Blok's model [7]. They calculated the average temperature at interface of tool and chip by considering uniform distribution of heat at tool-chip interface which is obviously not correct as the distribution of heat flux could not be uniform [25].

In 1955, Chao and Trigger [22] addressed this inconsistency by developing an analytical model by considering non-uniform distribution of heat flux both at chip and tool side. The concept of non-uniformity was further validated by Komanduri and Hou [25]. Chao and Trigger [22] started to solve the problem using the functional analysis method and found it difficult and time consuming. After this they tried a different approach called discrete numerical iterative method [22], still they found it tedious and time consuming. For the sake of simplicity, they moved further with a hybrid approach of using Jaeger's solutions with discrete numerical iterative method [22] i.e. a combination of analytical and numerical process. Though, the method solves the problem by giving uniformity in distribution of temperature at chip and tool, yet unsatisfactory results are predicted.

Komanduri and Hao [25] proposed another solution of the issue by modifying Jaeger’s solution of moving band heat source for chip side (Fig.20) and stationary rectangular heat source for tool side (Fig.21) along with the effect of additional boundaries and non-uniform distribution of heat partition fraction using functional analysis.

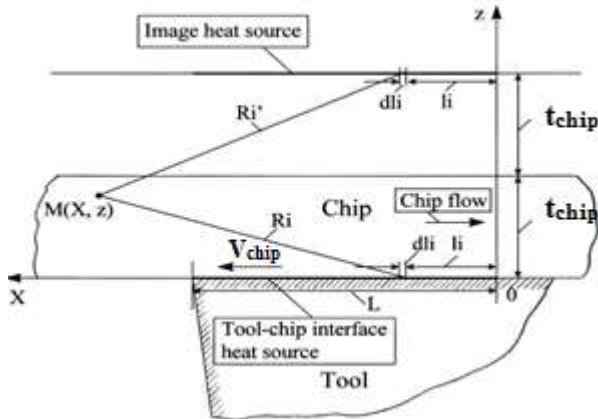


Fig. 20 Schematic showing the heat transfer model for the frictional heat source at the tool-chip interface on the chip side considering as a moving-band heat source problem [25]

The temperature rise at any point M(X, z) on chip side due to secondary heat zone was arrived as equation (9):

$$\theta_{chip-secondary} = \frac{q_{shear}}{\pi k_{chip}} \left\{ (B_1 - \Delta B) \int_{l_i=0}^l e^{-\frac{V_{chip}(X-l_i)}{2a_{chip}}} \left[K_0 \left(\frac{R_i V_{chip}}{2a_{chip}} \right) + K_0 \left(\frac{R_i' V_{chip}}{2a_{chip}} \right) \right] dl_i + 2\Delta B \int_{l_i=0}^l \left(\frac{l_i}{l} \right)^m e^{-\frac{V_{chip}(X-l_i)}{2a_{chip}}} \left[K_0 \left(\frac{R_i V_{chip}}{2a_{chip}} \right) + K_0 \left(\frac{R_i' V_{chip}}{2a_{chip}} \right) \right] dl_i + C\Delta B \int_{l_i=0}^l \left(\frac{l_i}{l} \right)^k e^{-\frac{V_{chip}(X-l_i)}{2a_{chip}}} \left[K_0 \left(\frac{R_i V_{chip}}{2a_{chip}} \right) + K_0 \left(\frac{R_i' V_{chip}}{2a_{chip}} \right) \right] dl_i \right\}$$

$$R_i = \sqrt{(X - l_i)^2 + z^2} \text{ and } R_i' = \sqrt{(X - l_i)^2 + (2t_{chip} - z)^2} \quad (9)$$

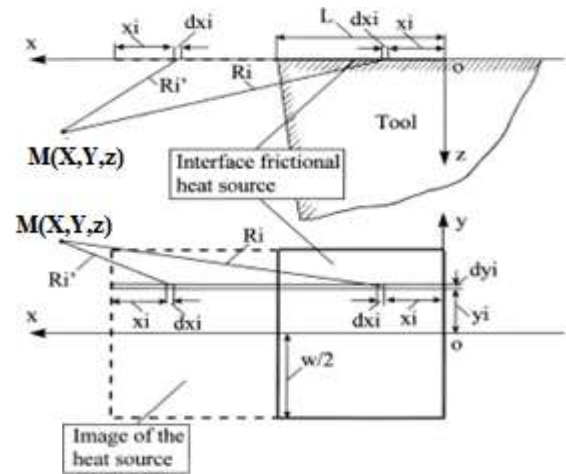


Fig.21 Schematic showing the heat transfer model of the frictional heat source at the tool-chip interfaces on the tool side considering as a stationary rectangular heat source problem [25]

The temperature rise at any point M(X,Y, z) on tool side due to secondary heat zone was found as:

$$\theta_{tool-secondary} = \frac{q_{shear}}{2\pi k_{tool}} \left\{ (1 - B_1 + \Delta B) \int_{y_i=-b_0}^{b_0} dy_i \int_{x_i=0}^L \left(\frac{1}{R_i} + \frac{1}{R_i'} \right) dx_i - 2\Delta B \int_{y_i=-b_0}^{b_0} dy_i \int_{x_i=0}^L \left(\frac{l_i}{L} \right)^m \left(\frac{1}{R_i} + \frac{1}{R_i'} \right) dx_i - C\Delta B \int_{y_i=-b_0}^{b_0} dy_i \int_{x_i=0}^L \left(\frac{l_i}{L} \right)^k \left(\frac{1}{R_i} + \frac{1}{R_i'} \right) dx_i \right\}$$

Where,

$$R_i = \sqrt{(x - x_i)^2 + (Y - y_i)^2 + z^2} \quad , \quad \text{and} \quad R_i' = \sqrt{(X - 2L + x_i)^2 + (Y - y_i)^2 + z^2} \quad (10)$$

Tool wear and coolant effects were not accounted for in equation (10). It limits its applicability to unrealistic conditions. To address this, a parameter ‘n’ (0<n<1) was introduced by Komanduri and Hou [25]. The modified equation (11) for real conditions is expressed as:

$$\theta_{tool-secondary} = \frac{q_{secondary}}{2\pi k_{tool}} \left\{ (1 - B_1 + \Delta B) \int_{y_i=-b_0}^{b_0} dy_i \int_{x_i=0}^L \left(\frac{1}{R_i} + \frac{n}{R_i'} \right) dx_i - 2\Delta B \int_{y_i=-b_0}^{b_0} dy_i \int_{x_i=0}^L \left(\frac{l_i}{L} \right)^m \left(\frac{1}{R_i} + \frac{n}{R_i'} \right) dx_i - C\Delta B \int_{y_i=-b_0}^{b_0} dy_i \int_{x_i=0}^L \left(\frac{l_i}{L} \right)^k \left(\frac{1}{R_i} + \frac{n}{R_i'} \right) dx_i \right\} \quad (11)$$

Using equation (9) and (11), and Blok’s [7] heat partition fraction and considering z=0, local and average temperature rise on both chip and tool due to secondary heat source can be determined.

Huang and Liang model for tool side:

Huang and Liang [21] recently developed a model (Fig.22) by taking following major considerations:

- (a) The interface boundary as adiabatic, and the tool clearance face as an insulated boundary
- (b) For simplification, ignored the rake angle effect, and cutting wedge angle as 90°
- (c) Two main imaginary heat sources FF and GG (Fig.22)
- (d) The heat intensity of the imaginary heat source FF is the same as that of the secondary heat source and the heat intensity of the imaginary heat source GG is double that of the secondary heat source.

The expression developed for total temperature rise at any point M(X, Y, z) on the tool side is given as equation (12):

$$\theta_{\text{tool-secondary}}(X, Y, z) = \frac{1}{2\pi k_{\text{tool}}} \int_0^l [1 - B_1(x)] q_{\text{secondary}}(x) dx \int_{-w/2}^{w/2} \left(\frac{1}{R_i} + \frac{1}{R_i'} \right) dy$$

Where,

$$R_i = \sqrt{(X - x)^2 + (Y - y)^2 + z^2} \text{ and}$$

$$R_i' = \sqrt{(X - 2l + x)^2 + (Y - y)^2 + z^2} \quad (12)$$

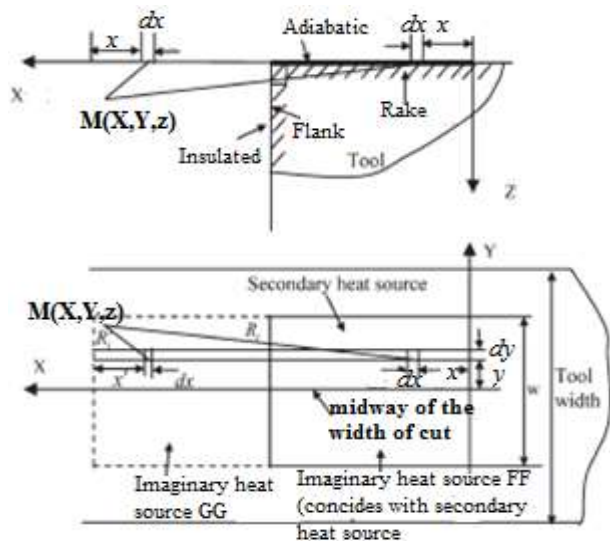


Fig.22 Huang and Liang heat transfer model of secondary heat source for tool side [21]

Huang and Liang model for chip side

A schematic of the heat transfer model proposed by Huang and Liang [21] for non-uniform secondary heat source to the chip side is shown in Fig.23. The model is similar to the model developed by Komanduri and Hou [25] except the following considerations:

- (a) Adiabatic interface, and insulated upper surface of the chip,
- (b) Three main imaginary heat sources CC, DD, and EE based on the method of images [9].
- (c) Heat source CC has the same intensity as the secondary heat source, while DD and EE have double that the intensity of secondary heat source.

The temperature rise on the chip side due to the secondary heat source can be modeled as the effect of non-uniform band heat sources moving at the chip velocity according to equation (13).

$$\theta_{\text{chip-secondary}} = \frac{1}{\pi k_{\text{chip}}} \int_0^l B_1 q_{\text{secondary}}(x) e^{-\frac{(x-x)V_{\text{chip}}}{2a_{\text{chip}}}} \left[K_0 \left(\frac{R_i V_{\text{chip}}}{2a_{\text{chip}}} \right) + K_0 \left(\frac{R_i' V_{\text{chip}}}{2a_{\text{chip}}} \right) + K_0 \left(\frac{R_i'' V_{\text{chip}}}{2a_{\text{chip}}} \right) \right] dx$$

Where,

$$R_i = \sqrt{(X - x)^2 + z^2},$$

$$R_i' = \sqrt{(X - x)^2 + (2t_{\text{chip}} - z)^2} \text{ and}$$

$$R_i'' = \sqrt{(X - x)^2 + (2t_{\text{chip}} + z)^2} \quad (13)$$

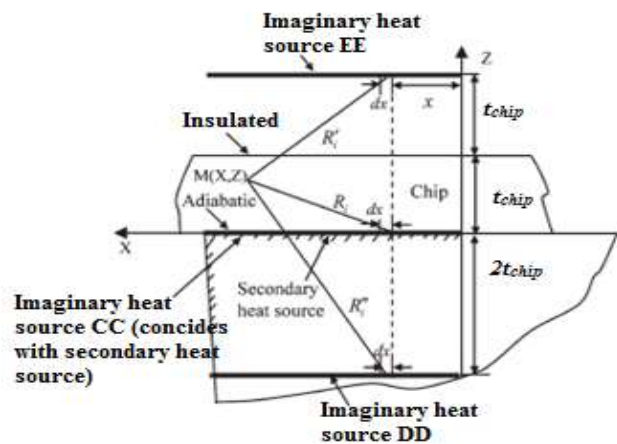


Fig.23 Huang and Liang heat transfer model of secondary heat source for chip side [21]

IV. Study of temperature rise due to Tertiary Deformation Zone

Prior to Huang and Liang, no major work was reported on the temperature rise due to tertiary deformation zone in the literature surveyed. They developed the temperature rise distribution measurement model for both work piece side and tool side, discussed in IV.I and IV.II respectively.

IV.I Huang and Liang model for work piece side

Huang and Liang [21] developed the model (Fig.24) by accounting the effect of tertiary heat source with following major considerations:

- (a) Heat source is moving in semi-infinite medium with cutting velocity
- (b) Insulated boundary conditions for the work piece surface
- (c) An imaginary heat source II with the same heat intensity as that of the tertiary heat source [9].

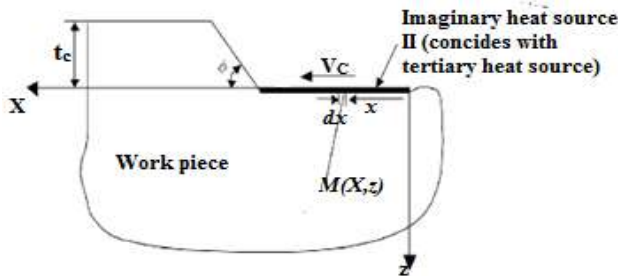


Fig.24 Huang and Liang heat transfer model of tertiary heat source relative to the work piece side [21]

Temperature rise on the part of work piece in contact with the tool worn flank face due to tertiary heat zone can be expressed as equation (14):

$$\theta_{work\ piece-tertiary}(X, z) = \frac{1}{\pi k_{work\ piece}} \int_0^{VB} B_2 q_{tertiary}(x) e^{-(X-x)V_c/(2a_{work\ piece})} \{K_0 \left[\frac{V_c}{2a_{work\ piece}} \sqrt{(X-x)^2 + z^2} \right] dx \quad (14)$$

IV.II Huang and Liang model for tool side

Major considerations accounted in the model (Fig. 25) [21] are as:

- (a) Both interface boundaries are adiabatic,
- (b) Two main imaginary heat sources JJ and KK [9]
- (c) The heat intensity of the imaginary heat source JJ is equivalent to that of the tertiary heat source, and the heat intensity of the imaginary heat source KK is twice the tertiary heat source.

The temperature rise at any point M(X, Y, z) on the tool side due to tertiary is expressed as equation (15).

$$\theta_{tool-tertiary}(X, Y, z) = \frac{1}{2\pi k_{tool}} \int_0^{VB} [1 - B_2] q_{tertiary}(x) dx \int_{-w/2}^{w/2} \left(\frac{1}{R_i} + \frac{1}{R_i'} \right) dy$$

Where,

$$R_i = \sqrt{(X-x)^2 + (Y-y)^2 + z^2} \text{ and } R_i' = \sqrt{(2VB - X - x)^2 + (Y-y)^2 + z^2} \quad (15)$$

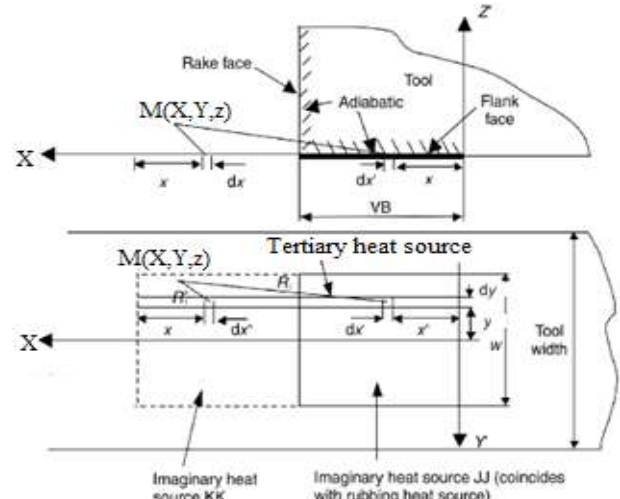


Fig.25 Huang and Liang heat transfer model of tertiary heat source relative to the tool side [21]

V. Study of temperature rise due to combined effect of Primary and Secondary Deformation zone

Prior to Komanduri and Hou, no major work was reported on the effect of combined heat source. Komanduri and Hou [26] were probably the first to study the combined effect of primary and secondary heat zone. Subsequently, Huang and Liang [20], [21] were the first to study the combined effect of all three heat sources.

Komanduri and Hou's model for combined effect of primary and secondary heat zones

In order to obtain the combined effect of primary heat zone and secondary heat zone, Komanduri and Hou proposed that the individual effect of primary heat zone and secondary heat zone may be superimposed, if both are calculated on common co-ordinate system. The model [26] is explained in Fig.26. The pertaining equation (16) is as:

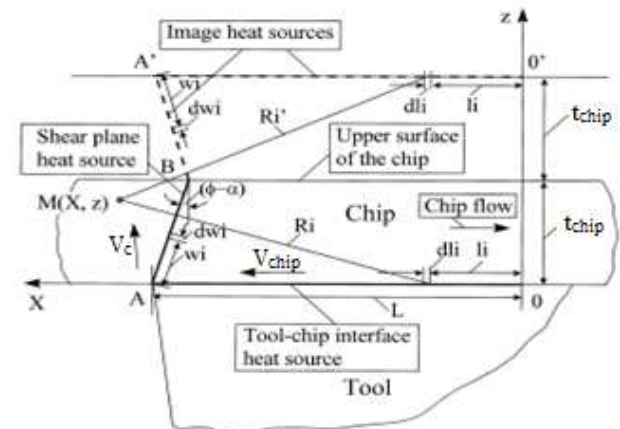


Fig.26 Schematic of Komanduri and Hou's heat transfer model with a common coordinate system for the combined effect of two principal heat sources - the shear plane heat source and the tool-chip interface frictional heat source [26]

VI. Conclusion

At the end of the paper following observations can be made:

1. Form observation of comparative study of merits and demerits of experimental methods available in literature, it is evident that still we are in search of a perfect technique which is economic and implementable to all materials in all respects.
2. The combined effect of two or three deformation zone from primary, secondary, and tertiary on temperature rise may be closely approximated by simply superimposing their individual effects in a common co-ordinate system.
3. Results of Komanduri and Hou & Huang and Liang are very close to reality; however, they are obtained from different approaches.
4. Some input parameters in Komanduri and Hou model for Secondary deformation zone is based on hit and trail, while no such hit and trail data is used by Huang and Liang. Though, their results are similar and in close conformation with the experimental results.
5. Tertiary deformation zone do not add much in temperature rise, and left unaccounted by majority of researchers but in the time of modern computing this minor effect may be studied thoroughly individually

and in combination with the effect of other zone(s) in or other direction(s) shown by Huang and Liang.

VII. Scope of further work

From the above study the scope of further work identified by the authors are as under:

1. In present era of modern computing, the availability of economic and powerful computers, hardly any method could be tedious and time consuming. In fact, approaches rejected earlier on the ground of tedious and lengthy calculations should be relooked. Some of them may be more convenient and time saving than most numerical methods used earlier.
2. A lack of diversification in cutting parameters is observed in validation of modeling equations. For generalization of modeling equation, the models must be tested with a variety of machining parameters.
3. The values of some constants used in Komanduri and Hou's model as well as in Huang and Liangs' Model are to be approximated by trial and error method. Efforts could be made to develop a general and simplified relation to obtain the value of these constants by giving some input parameters.
4. Tool flank contact length as used in few of Huang and Liangs' Models is still measured experimentally; there is a scope for development of a mathematical relation to calculate tool flank contact length.

TABLE 1
COMPARATIVE STUDY OF MERITS AND DEMERITS OF VARIOUS EXPERIMENTAL TECHNIQUES

S. No.	Technique		Major Merits	Major Demerits	Remarks (if any)
1	Thermal paint [27,28]		Simplest and economical	Not very accurate and prone to errors	Result verification by any other accurate enough technique is recommended
2	Thermocouple	Tool-work [29]	Ease of experimental setup	For making observation at different point, setup is required to rearranged after stopping the machining	1. Calibration of tool-work piece pair is difficult 2. Limited transient response time
		Transverse [30]	Capable of notifying temperature at various points	Cannot be used for processes like grinding, drilling, milling, etc.	
		Embedded [31]	Can be used for processes like grinding, drilling, milling, etc.	1. Temperature of surface cannot be measured directly 2. Destructive technique	
3	Pyrometer	Infrared radiation [32,33]	1. Faster results 2. Can be used for any surface	1. Emissivity of body (under consideration) keeps on changing and hence affects the results 2. The complete isotherms cannot be plotted for every machining material	1. Photo cell is sensitive to change in ambient temperature, and IR 2. Destructive technique
		Optical Infrared radiation [34,35,36]			
4	Infrared photographic [37,38]		1. Very fast response 2. Can be used in hazardous conditions	1. Requires preheating 2. Very expensive	Readings can be taken directly and long lasting
5	Fine powder [39]		Economic	Not reliable , results are obtained in approximate temperature range	No need for calibration
6	Metallographic [40]		Accuracy $\pm 25^{\circ}\text{C}$ in the range of 650°C to 900°C	1. Can be used only for specific materials only (HSS) 2. High cutting speed 3. Rapid tool breakage	Requires calibration

TABLE 2
EXPLANATIONS FOR ABBREVIATIONS USED

Abbreviations	Details	Source	Unit
θ_M	Temperature rise at concerned point M due to moving band heat source	Refer equation (3,4,6,7,17)	$^{\circ}\text{C}$
$\theta_{\text{avg-chip}}$	Average value of temperature rise on chip side	Refer equation (1,2)	$^{\circ}\text{C}$
$\theta_{\text{chip-ahcar}}$	Temperature rise at concerned point due to primary heat zone on chip side	Refer equation (8)	$^{\circ}\text{C}$
$\theta_{\text{work piece-ahcar}}$	Temperature rise at concerned point due to primary heat zone on work piece side	Refer equation (9)	$^{\circ}\text{C}$
$\theta_{\text{chip-secondary}}$	Temperature rise at concerned point due to secondary heat zone on chip side	Refer equation (10,14)	$^{\circ}\text{C}$
$\theta_{\text{tool-secondary}}$	Temperature rise at concerned point due to secondary heat zone on chip side	Refer equation (11,12,13)	$^{\circ}\text{C}$
$\theta_{\text{tool-tertiary}}$	Temperature rise at concerned point due to tertiary heat zone on tool side	Refer equation (16)	$^{\circ}\text{C}$
$\theta_{\text{work piece-tertiary}}$	Temperature rise at concerned point due to tertiary heat zone on work piece side	Refer equation (15)	$^{\circ}\text{C}$
A	Percentage of total shearing deformation energy appearing as sensible heat	87.5 approx	%
t_c	Undeformed chip thickness	= depth of cut	cm
t_{chip}	Deformed chip thickness	Experimental (vertical profile projector)	cm
R	Chip thickness ratio	t_c/t_{chip}	--
α	Rake angle	Tool specifications	Degree
ϕ	Shear angle	$\tan^{-1} \frac{r \cos \alpha}{\lambda \cos \phi}$	Degree
β	Friction angle	$\tan^{-1} \left(\frac{F_f}{N} \right)$	degree
F_c	Cutting force	Experimental (dynamometer)	N
F_f	Feed force	Experimental (dynamometer)	N
F_r	Radial force	Experimental (dynamometer)	N
F_{xy}	Resultant of feed force and radial force	$\sqrt{(F_f^2 + F_r^2)}$	N
F_s	Shear force	$F_c \cos \phi - F_{xy} \sin \phi$	N
F_{ns}	Normal to shear force	$F_c \sin \phi + F_{xy} \cos \phi$	N
F	Frictional force	$F_c \sin \alpha + F_{xy} \cos \alpha$	N
N	Normal to frictional force	$F_c \cos \alpha - F_{xy} \sin \alpha$	N
V	Moving band heat source velocity		cm/s
V_x	Moving band heat source velocity along oX axis		cm/s
V_c	Cutting velocity	Experimental (DRO/CNC machine)	cm/s
V_{chip}	Chip velocity	$\frac{V_c \sin \phi}{\cos(\phi - \alpha)}$	cm/s
V_s	Shear velocity	$\frac{V_c \cos \alpha}{\cos(\phi - \alpha)}$	cm/s
L_{sb}	Length of shear plane	$t_c / \sin \phi$	cm
L	Width of shear band heat source	--	cm
L	Tool chip contact length	$\frac{t_c \sin(\phi + \theta - \alpha)}{\sin \theta \cos \phi}$	cm
VB	Flank wear length	--	cm
W	Width of chip	Digital Vernier Calliper	cm
K	Thermal conductivity	Data book	J/cms $^{\circ}\text{C}$
k_{chip}	Thermal conductivity of chip	Data book	J/cms $^{\circ}\text{C}$
$k_{\text{work piece}}$	Thermal conductivity of work piece	Data book	J/cms $^{\circ}\text{C}$
k_{tool}	Thermal conductivity of tool	Data book	J/cms $^{\circ}\text{C}$
A	Thermal diffusivity	Data book	cm 2 /s
a_{chip}	Thermal diffusivity of chip	Data book	cm 2 /s
$a_{\text{work piece}}$	Thermal diffusivity of work piece	Data book	cm 2 /s
a_{tool}	Thermal diffusivity of tool	Data book	cm 2 /s
$B_{\text{work piece}}$	Fraction of shear plane heat transferred to work piece	--	--
B_{chip}	Fraction of shear plane heat transferred to chip	--	--
$B_1(x)$	Fraction of secondary heat source transferred to chip	--	--
$B_2(x)$	Fraction of tertiary heat source transferred to work piece	--	--
ΔB	Maximum compensation of B_{chip} at two ends of the interface heat source	--	--
Abbreviations	Details	Source	Unit

K_0	Modified Bessel's function of second kind of order zero	--	--
O	Origin of moving co-ordinate system	--	--
X,Y,z	The co-ordinate of the point where the temperature rise is to be measured in moving co-ordinate system	--	--
ϕ	Oblique angle	--	Degree
M,k',C	Constants	By trial and error	
Q_{primary}	Heat intensity of the primary heat source	$\frac{r_0 \sqrt{v}}{L_0 \sqrt{v}}$	J/cm ² s
$Q_{\text{secondary}}$	Heat intensity of the secondary heat	$\frac{r_0 \sqrt{v}}{L_0 \sqrt{v}}$	J/cm ² s
Q_{tertiary}	Heat intensity of the tertiary heat	--	J/cm ² s
ρ	Density	Data book	gm/cc
C	Specific heat	Data book	J/gm ⁰ C
J	Mechanical Equivalent of Heat	Data book	J/calorie
R	Distance between infinitely small element on moving line heat source and the point M, where temperature rise is concerned	--	Cm

REFERENCES

[1] Thompson B. Count Rumford, 1798, An inquiry concerning the source of heat which is excited by friction, Philosophical Transactions of the Royal Society of London; 18:278-87.

[2] Joule JP., 1850, Mechanical equivalent of heat, Philosophical Transactions of the Royal Society of London; 61-81

[3] Taylor, G.I. and Quinney, H., 1934, The Latent Energy Remaining in a Metal after Cold Working, Proc. Roy. Soc. A, 143, 307-326

[4] A.B. Chattopadhyay, Cutting temperature causes effects, assessment and control. MHRD NEPTel Manufacturing Science II, Lecture 11, IIT Kharagpur Version 2.

[5] Lei Pang, 2012, Analytical modeling and simulation of metal cutting forces for engineering alloys: Ph.D. thesis, department of Engineering and Applied Science, University of Ontario Institute of Technology, page 8

[6] Rosenthal D., 1946, The theory of moving sources of heat and its application to metal treatments, Transactions of ASME; 68: 849-66

[7] Blok H., 1938, Theoretical study of temperature rise at surfaces of actual contact under oiliness lubricating conditions. Proceedings of General Discussion on Lubrication and Lubricants, Institute of Mechanical Engineers London., pg. 222-235.

[8] Jaeger JC., 1942, Moving sources of heat and the temperature at sliding contacts. Proceedings of the Royal Society of NSW; 76 : 203-24

[9] Carslaw HS, Jaeger JC., 1959, Conduction of heat in solids. Oxford, UK: Oxford University Press.

[10] Loewen EG, Shaw MC., 1954, On the analysis of cutting tool temperatures, Transactions of ASME; 71: 217-31

[11] Cook NH et al., 1954, Discontinuous chip formation. Transactions of the ASME; 76: 153-62

[12] Leone WC., 1954, Distribution of shear-zone heat in metal cutting, Transactions of ASME; 76: 121-5

[13] Weiner JH., 1955, Shear plane temperature distribution in orthogonal machining, Transactions of ASME; 77: 1331-41

[14] Hahn RS., 1951, On the temperature developed at the shear plane in the metal cutting process. Proceedings of First U.S. National Congress of Applied Mechanics pg. 661-6

[15] Dutt RP, Brewer RC., 1964, On the theoretical determination of the temperature field in orthogonal machining. International Journal of Production Research; 4:91-114

[16] Dawson PR, Malkin S., 1984, Inclined moving heat source model for calculating metal cutting temperatures. Transactions of ASME; 106: 179-86

[17] Chao BT, Trigger KJ., 1953, The significance of thermal number in metal machining, Transactions of ASME; 75: 109-20

[18] Trigger KJ, Chao BT., 1951, An analytical evaluation of metal cutting temperature, Transactions of ASME; 73: 57-68

[19] R. Komanduri, Z.B. Hou, 2005, Thermal modeling of the metal cutting process Part I - Temperature rise distribution due to shear plane heat source, International Journal of Mechanical Sciences 2000; 42: 1715-52

[20] Y. Huang, S. Liang, Cutting temperature modeling based on non-uniform heat intensity and partition ratio, Taylor and Francis, Machining Science and Technology, 9: 301-323

[21] Y. Huang and S. Liang, Modelling of the cutting temperature distribution under the tool flank wear effect

[22] Chao BT, Trigger KJ., 1955, Temperature distribution at the tool-chip interface in metal cutting, Transactions of the ASME; 72: 1107-21

[23] Chao BT, Trigger KJ., 1958, Temperature distribution at the tool-chip and tool-work interface in metal cutting, Transactions of the ASME; 80: 311-20

[24] Nakayama K., 1956, Temperature rise of work piece during metal cutting, Bulletin of the Faculty of Engineering, Yokohama National University, Yokohama, Japan; 5: 1

[25] R. Komanduri, Z.B. Hou, 2001, Thermal modeling of the metal cutting process - Part II: temperature rise distribution due to frictional heat source at the tool-chip interface, International Journal of Mechanical Sciences; 43: 57-88

[26] R. Komanduri, Z.B. Hou, 2001, Thermal modeling of the metal cutting process - Part III: temperature rise distribution due to the combined effects of shear plane heat source and the tool-chip interface frictional heat source, International Journal of Mechanical Sciences; 43: 89-107

[27] Schallbroach H, Lang M., 1943, Messung der Schnitttemperaturmittels Temperaturanzeigender Farbanstriche. Zeitschrift des Vereines Deutscher Ingenieure ;87:15-9.

[28] Bickel E, Widmer W. 1954, Die Temperaturen an der Werkzeugschneide. Zurich, Switzerland: Industrielle Organization.

[29] L.B. Abhang and M. Hameedullah., 2010, Chip-tool interface temperature prediction model for turning process. International Journal of Engineering Science and Technology Vol. 2(4), 382-393

[30] Kraemer G. 1936, Neitrag zur Erkenntnis der beim Drehenaufretenden Temperaturen und deren Messung mit einem Gesamtstrahlungsempfänger. Dissertation, Hannover.

[31] A.B. Chattopadhyay, Cutting temperature causes, effects, assessment and control. MHRD NEPTel Manufacturing Science II, Lecture 11, IIT Kharagpur Version 2. Page 9

[32] Schwerd F., 1933, Ueber die Bestimmung des Temperaturfeldes beim Spanablauf (Determination of the Temperature Distribution During Cutting). Z VDI; 9:211.

[33] Kraemer G., 1936., Neitrag zur Erkenntnis der beim Drehenaufretenden Temperaturen und deren Messung mit einem Gesamtstrahlungsempfänger. Dissertation, Hannover.

[34] Lenz E., 1963, Der Einfluss der Schnitttemperatur auf die Standzeit der keramischen Schneidstoffe. Maschinenmarkt; 28:30.

[35] Friedman MY, Lenz E., 1971, Determination of temperature field on upper chip surface. Annals of CIRP; 19:395-8.

[36] Ueda T, Hosokawa A, Yamamoto A., 1985, Studies on temperature of abrasive grains in grinding — application of infrared radiation pyrometer. Trans ASME, J of Engg for Ind; 107:127-33.

[37] Boothroyd G., 1961, Photographic techniques for the determination of metal cutting temperatures. Brit J of Appl Physics; 12:238-42.

[38] Jeelani S., 1981, Measurement of temperature distribution in machining using IR photography. Wear; 68:191-202.

[39] Kato S, Yamaguchi K, Watanabe Y, Hiraiwa Y., 1976, Measurement of temperature distribution within tool using powders of constant melting point. Trans ASME, J of Engg for Ind; 108:607-13.

[40] Wright PK, Trent EM., 1973, Metallographic methods of determining temperature gradients in cutting tools. J Iron and Steel Institute; 211:364-88.